ANSP-M-8
FEBRUARY 1974
Copy No. 55

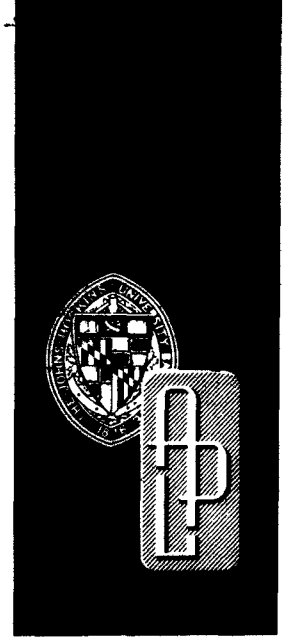

Aerospace Nuclear Safety Program

ORBITAL LIFETIME ESTIMATES

By L. L. PERINI

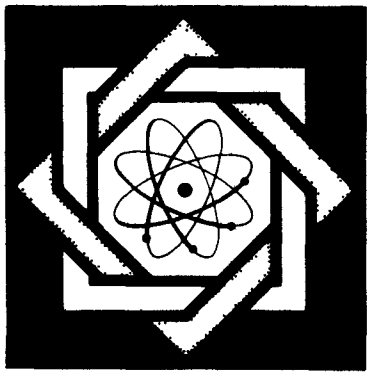

DISCLAIMER

LEGIBILITY NOTICE

A major purpose of the Technical Information Center is to provide the broadest possible dissemination of information contained in DOE's Research and Development Reports to business, industry, the academic community, and federal, state, and local governments. Non-DOE originated information is also disseminated by the Technical Information Center to support ongoing DOE programs.

Although large portions of this report are not reproducible, it is being made available only in paper copy form to facilitate the availability of those parts of the document which are legible. Copies may be obtained from the National Technical Information Service. Authorized recipients may obtain a copy directly from the Department of Energy's Technical Information Center.

ANSP-M--8

DE88 012306

ANSP-M-8

FEBRUARY 1974

Aerospace Nuclear Safety Program

ORBITAL LIFETIME ESTIMATES

By L. L. PERINI

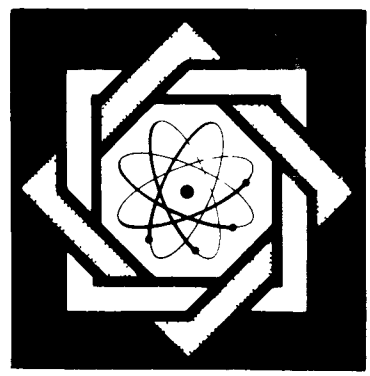

THE JOHNS HOPKINS UNIVERSITY • APPLIED PHYSICS LABORATORY
8621 Georgia Avenue ◦ Silver Spring, Maryland ◦ 20910

THE JOHNS HOPKINS UNIVERSITY
APPLIED PHYSICS LABORATORY
SILVER SPRING MARYLAND

FOREWORD

The work reported herein was conducted by the Applied Physics Laboratory Aeronautics Division for the Atomic Energy Commission, Safety Branch, Space Nuclear Systems Office. Activities of the Aeronautics Division are under the general supervision of Dr. William H. Avery. The Project Engineer for the Aerospace Nuclear Safety Program is James C. Hagan.

THE JOHNS HOPKINS UNIVERSITY
APPLIED PHYSICS LABORATORY
SILVER SPRING, MARYLAND

ABSTRACT

Orbital lifetime estimates for long lifetimes ($>$ 30 years) are presented for initial eccentricities from 0 to 0.95 and for perigee altitudes from 200 to 1600 km. The lifetime estimates are based on a semi-analytic form of the equations of motion developed by King-Hele and the latest (1971) Jacchia atmospheric model. A mean 11 year solar cycle based on historical records of the Zurich sunspot number is employed in the calculations. Comparisons are made to previously published lifetime charts.

THE JOHNS HOPKINS UNIVERSITY
APPLIED PHYSICS LABORATORY
SILVER SPRING MARYLAND

SUMMARY

An economical scheme for estimating orbital lifetime, including the effect of long term variations in solar activity, has been developed. The study was principally directed toward providing estimates of the lifetime for long terms (tens and hundreds of years) and accordingly simplifications were employed in order to reduce the computational expense. The lifetime computational code that has been developed is both small and inexpensive to employ. The computer program employs a semi-analytic form of the equation of motion (King-Hele) and the latest (1971) Jacchia atmosphere model. The time variation of solar activity that established the upper atmosphere density used for the calculations is based on historical data which extend to the previous 10 solar cycles. (Each solar cycle is 11 years in length.)

The results of this study indicate that:

1. Using a mean solar cycle as a basis, lifetimes are a factor of 3 to 4 greater than would be predicted using the 1962 U. S. Standard Atmosphere.

2. For long lifetimes ($>$ 30 years), the lifetime estimate is independent of where on the solar cycle the calculations are begun.

3. For long lifetimes ($>$ 30 years), the lifetime is directly proportional to ballistic coefficient.

4. A one sigma deviation of the solar cycle from its mean value can affect the lifetime by a factor of $\sim$ 1.5.

5. Long (> 30 years) lifetime estimates based on a constant exospheric temperature, derived from a value of density which is time averaged over the solar cycle, are good approximations to more exact calculations that directly employ a time-varying solar activity.

This conclusion permitted the economical development of an orbital lifetime chart that is valid for estimating lifetimes in excess of 30 years.

6. Lifetime estimates based on a mean solar cycle are, in general, significantly higher than lifetime estimates from the Design Guide to Orbital Flight handbook, which has been the basis for the current LES 8/9 mission safety analyses.

TABLE OF CONTENTS

LIST OF FIGURES

LIST OF TABLES

THE JOHNS HOPKINS UNIVERSITY
APPLIED PHYSICS LABORATORY
SILVER SPRING, MARYLAND

I. INTRODUCTION

Orbital lifetime estimates for satellites is of primary concern for a comprehensive safety analysis of thermoelectric nuclear power supplies employed on spacecraft. Current lifetime estimates are normally based on lifetime charts as found, for example, in Ref. 1. These charts, however, are based on a 'standard' atmosphere and do not account for the large variations in upper atmosphere properties resulting from solar activity. More accurate estimates are made by employing computer programs[2] that employ numerical integration of the equations of motion along the orbit and account for solar and lunar geopotential influences and atmospheric variations due to geomagnetic and solar activity. The computer programs are quite sophisticated, having the capability of accounting for daily variations in atmospheric properties. For long term predictions ($\lesssim$ 100 years), however, it is found that the principal uncertainty is the unpredictability of the major influence of the atmospheric properties--the long term, 11 year, solar cycle. With this uncertainty then, it does not appear justified to employ a sophisticated and costly model for long lifetime estimates since the results will still be inaccurate due to the lack of accuracy in the basic input data.

With these considerations, it was decided to employ a semi-analytic procedure and to develop a simple and efficient computer code

directed toward long lifetime estimates ($\gtrsim$ 100 years) accepting some inaccuracies in the solution of the equations of motion as being compatible with the degree of uncertainty of solar activity predictions.

The semi-analytic technique employed for the trajectory is outlined in Section II, the atmospheric model is presented in Section III, the relationship of solar and geomagnetic phenomena to the atmospheric model is discussed in Section IV, the 11 year solar cycle model is covered in Section V and the results and conclusions are presented in Sections VI and VII, respectively.

II. EQUATIONS OF MOTION

The numerical procedure employed in the analysis is based on the development presented by King-Hele.[3] Before presenting the major features, however, it should be noted that the following assumptions are employed:

(1) The atmosphere is spherically symmetrical.

(2) Air density varies exponentially with height.

(3) Lunar-solar perturbations are neglected.

(4) The only nonconservative force considered is air drag and it acts in a direction tangent to the orbital plane, i.e., normal forces are neglected.

(5) During one revolution, the action of air drag changes the orbit by a small amount, where squares can be neglected.

(6) The unperturbed orbit is an exact ellipse.

(7) The atmosphere rotates with constant angular velocity, ω.

(8) The atmospheric density does not vary with time. This assumption is involved in the derivation of the equations of motion, however, long term variations are considered in a corrective manner by reevaluation of the density scale height.

Lagranges planetary equations for the change in the orbital elements due to external nonconservative forces are given by

$$\frac{da}{dt} = 2 \frac{a^2 v}{\mu} f_T \tag{1}$$

$$\frac{de}{dt} = \frac{1}{v} \left\{ 2 f_T (e + \cos \theta) - f_N \frac{r}{a} \sin \theta \right\} \tag{2}$$

where f_T and f_N are the components of the total force tangent and normal, respectively, to the orbit in the orbital plane. The force under consideration is a drag force related to the drag coefficient.

$$D = \rho V^2 S \, C_D/2 \tag{3}$$

The velocity V is the velocity of the satellite relative to the ambient air and in terms of the satellite inertial velocity v and the air velocity, V_A,

$$V = (v^2 + V_A{}^2 - 2v \, V_A \cos \gamma)^{1/2} \tag{4}$$

where γ is the angle between the satellite velocity vector $\bar{v}$ and the local horizontal (which is parallel to the air velocity vector $\bar{v}_A$). The air velocity can be written in terms of the angular velocity about the earth's center as,

$$V_A = r\omega \cos \phi \tag{5}$$

where ϕ is the geocentric latitude and r is the distance from the earth's center. Assuming that γ', the angle between $\bar{V}_A$ and the horizontal component of $\bar{v}$, is small, we have

$$\cos \gamma \cos \phi = \cos i \tag{6}$$

where i is the inclination of the orbit plane. Neglecting $(r\omega)^2$ terms and assuming $r\omega \cos i/v \ll 1$ for the expansion, Eqs. (4)-(6) give

$$V = v - r\omega \cos i \tag{7}$$

As $r\omega/v$ is small it is assumed that the values at perigee can be used and also since i does not vary by a substantial amount during a satellite lifetime we use the initial value i_o,

$$V = v\left(1 - r_{p_o}\, \omega \cos i_o/v_{p_o}\right) \tag{8}$$

The resultant drag force is then

$$D = \rho v^2 FSC_D/2 \tag{9}$$

where

$$F = \left(1 - r_{p_o} \omega \cos i_o / v_{p_o}\right)^2 \tag{10}$$

In evaluating the force components it is assumed that the angle between $\overline{V}$ and $\overline{v}$ is small so that the total drag force is tangent to the orbit,

$$f_T = - D/m = - \rho v^2 FSC_D/(2m) \tag{11}$$

Defining the ballistic coefficient

$$\beta = m/(FSC_D) \tag{12}$$

Eq. (11) becomes,

$$f_T = - \rho v^2/(2\beta) \tag{13}$$

It should be noted that the ballistic coefficient defined by Eq. (12) includes the function F. For a nonrotating earth assumption ($\omega = 0$) and/or the orbit plane lying in the north-sound earth plane ($i_o = 90^o$), F = 1.0; however, for other cases, as pointed by King-Hele, the value of F can be as low as 0.88. We also assume that normal forces due to tumbling and/or flight attitudes giving rise to lift are zero so that

$$f_N = 0 \tag{14}$$

The equations of motion are then

$$\frac{da}{dt} = - \frac{a^2 \rho v^3}{\beta \mu} \tag{15}$$

$$\frac{de}{dt} = \frac{\rho v}{\beta} (e + \cos\theta) \tag{16}$$

Converting from the true anomaly to the eccentric anomaly E and integrating around the orbit we have for the changes in a and ae per revolution,

$$\Delta a = -\frac{a^2}{\beta} \int_0^{2\pi} \frac{(1 + e\cos E)^{3/2}}{(1 - e\cos E)^{1/2}} \rho \, dE \tag{17}$$

$$\Delta(ae) = -\frac{a^2}{\beta} \int_0^{2\pi} \left(\frac{1 + e\cos E}{1 - e\cos E}\right)^{1/2} (\cos E + e) \rho \, dE \tag{18}$$

For the air density ρ we employ the exponential variation

$$\rho = \rho_p \, e^{\frac{r_p - r}{H}} \tag{19}$$

where ρ_p is the density at perigee and r_p is the perigee distance from the earth's center. The constant H is termed the density scale height and assumed to remain constant in the analytic integrations. Since $r_p = a(1-e)$, Eq. (19) can be written as,

$$\rho = \rho_p \, e^{\frac{a_o - a - a_o e_o}{H}} \, e^{\frac{ae\cos E}{H}} \tag{20}$$

The integrands in Eqs. (17) and (18) are expanded with the binominal expansion. For $0 < e < 0.2$ the integrands are expanded in powers of e and for $0.2 \leq e \leq 1.0$ the integrands are expanded in powers of $1 - \cos E$. The case $e = 0$, circular orbits, follows from the e expansions with $e = 0$. The expansions are integrated term by term and truncated, resulting in

analytic representations of Δa and $\Delta(ae)$ per revolution. Derivations and final equations used in the computer code are documented in the Appendix.

The scale height H is, for a realistic atmosphere, not constant but varies with position (latitude, longitude and height) and time. Based on the results of King-Hele[3] the scale height is evaluated at $Z = 1.5Z_p$ for $e > 0.2$ and at $Z = Z_p(1 + 25e)$ for $e \leq 0.2$ to account for the change in height during the orbit. In addition the scale height is reevaluated whenever the perigee altitude changes by 10 km. The variations of H with time will be considered below when the Jacchia atmospheric model is discussed.

The above equations were programmed in PL/1 for the IBM 360/91 computer. In order to verify the accuracy of the method a series of orbital lifetimes were calculated employing tabular values of the 1962 standard atmosphere,[4] for which solutions are available[2] based on a complete numerical solution of the equations of motion. Five cases were run with a 5000 km apogee altitude and for perigee altitudes of 200, 250, 350, 450 and 550 km. The results of Ref. 2 are presented in graphical form on logarithmic plots and the resulting comparisons show a detectable difference at only one point, the 550 km case, where a difference of $\sim$ 8% is found. In view of the uncertainty in long term projection of the high altitude atmospheric properties to be discussed below it is felt that the present model is more than adequate in terms of accuracy.

The advantages of the calculation method described here are that the resulting computer program is small (i.e., manageable) and run times are short (i.e., low cost). The complete program consists of $\sim$ 200 source statements

and the cost on the IBM 360/91 is estimated as 12¢ per year lifetime, employing the Jacchia atmospheric model (Sect. III) and the 11 year mean solar cycle (Sect. V).

III. ATMOSPHERIC MODEL

Of primary concern for orbital lifetime studies are the atmospheric properties above 100 km. Below 100 km the lifetime of a satellite is essentially completed. Above 100 km the atmosphere is conveniently classified into two regions, the thermopause (100 km $<$ Z $<$ 450 km) and the exosphere (Z $>$ 450 km). The region above 100 km is commonly referred to as the 'upper atmosphere.' The mathematical model employed to describe the upper atmospheric properties is based on diffusion equilibrium assumptions, whereby the partial densities of the atmospheric constituents vary according to diffusion theory. The model is also based on 'static' assumptions, i.e., time dependent diffusional effects are neglected, and charged particles are neglected as they are insignificant in affecting density.

The atmospheric model relating density to altitude employed in this study is based on the method outlined by Jacchia.[5] The model is restricted to altitudes greater than 90 km. Between 90 and 100 km the barometric equation is used.

$$\rho = \rho_o \frac{\bar{m}}{\bar{m}_o} \frac{T_o}{T} \exp\left(- \int_{Z_o}^{Z} \frac{\bar{m} g}{RT} \, dz \right) \tag{21}$$

where

$$\overline{m} = \sum_{n=0}^{6} C_n (Z-90)^n \qquad (22)$$

$C_0 = 28.82678$ $\qquad C_1 = 7.40066 \times 10^{-2}$

$C_2 = 1.19407 \times 10^{-2}$ $\qquad C_3 = 4.51103 \times 10^{-4}$

$C_4 = 8.21895 \times 10^{-6}$ $\qquad C_5 = 1.07561 \times 10^{-5}$

$C_6 = -6.97444 \times 10^{-7}$

and the subscript 0 refers to the boundary conditions at 90 km.

Above 100 km the diffusion equation is employed,

$$\rho = \frac{1}{A} \sum_i m_i n_{i_y} \left(\frac{T}{T_y}\right)^{-(1+\alpha_i)} \exp\left[-\frac{m_i}{R} \int_{Z_y}^{Z} \frac{g}{T}\, dZ\right] \qquad (23)$$

where i refers to the chemical species, i = N_2, Ar, He, O, O_2 and H and the subscript y refers to the boundary conditions at Z_y = 100 km.

The acceleration due to gravity is approximated by

$$g = g_{SL} (1 + Z/R_e)^{-2} \qquad (24)$$

where g_{SL} = 9.8195 m/sec^2 and $R_e = 6.37815 \times 10^3$ km.

The temperature profiles are represented by two equations, the first applicable below Z_x = 125 km and the second above Z_x = 125 km,

$$90 \leq Z < 125 \text{ km}$$

$$\frac{T - T_x}{T_o - T_x} = (Z_x - Z)\left[0.05429 - 3.9650 \times 10^{-5} (Z_x - Z)^2 + 5.3311 \times 10^{-7} (Z_x - Z)^3\right] \quad (25)$$

$$Z > 125 \text{ km}$$

$$T = T_x + \frac{2}{\pi}(T_\infty - T_x) \tan^{-1}\left\{\frac{1.9\pi}{g} \frac{T_x - T_o}{T_\infty - T_x} \frac{Z - Z_x}{Z_x - Z_o}\left[1 + 4.5 \times 10^{-6} (Z - Z_x)^{2.5}\right]\right\} \quad (26)$$

where

$$T_x = 371.6678 + 0.0518806\, T_\infty - 294.3505 \exp(-0.00216222\, T_\infty) \quad (27)$$

The boundary conditions for Eqs. (21) and (23), respectively, are given by

@ $Z_o = 90$ km; $T_o = 183^\circ$K, $\bar{m}_o = 28.82678$, $\rho_o = 3.46 \times 10^{-9}$ g/cm^3

@ $Z_y = 100$ km; T_y is evaluated from Eq. (25) and the species number densities at Z_y are given by

$$\left.\begin{aligned} \eta_{N_2} &= 0.78110\, \bar{m}_x\, N/\bar{m}_{SL} \\ \eta_{Ar} &= 0.0093432\, \bar{m}_x\, N/\bar{m}_{SL} \\ \eta_{He} &= 6.1471 \times 10^{-6}\, \bar{m}_x\, N/\bar{m}_{SL} \\ \eta_O &= 2N(1 - \bar{m}_x/\bar{m}_{SL}) \\ \eta_{O_2} &= N(1.20955\, \bar{m}_x/\bar{m}_{SL} - 1) \end{aligned}\right\} \quad (28)$$

where $\overline{m}_{SL} = 28.9660$ and the total number of particles per unit volume, N, is

$$N = A\rho_y/\overline{m}_y \tag{29}$$

and $\overline{m}_y$ is evaluated from Eq. (22) at $Z = Z_y$. For hydrogen the number density is given by,

$$\log_{10} \eta_H = 73.13 - 39.40 \log_{10} T_{500} + 5.5 (\log_{10} T_{500})^2 \tag{30}$$

at Z = 500 km and T_{500} is the temperature, ^oK, at Z = 500 km evaluated from Eq. (26). Below 500 km η_H is neglected in evaluating Eq. (23). The thermal diffusion coefficients α_i are zero for all species except He for which $\alpha_{He} = 0.38$.

The integrals in Eqs. (21) and (23) are evaluated by the simple trapezoidal rule. For Eq. (21) a step size of $\Delta Z = 2$ km is employed. For Eq. (23) the step size varies with the altitude regime, $100 \leq Z \leq 125$ km, $\Delta Z = 1.923$ km; $125 \leq Z \leq 200$ km, $\Delta Z = 3.75$ km; $200 \leq Z \leq 300$ km, $\Delta Z = 5$ km and for $Z > 300$ km, $\Delta Z = 50$ km.

Results from the above equations where checked against tabular values listed in Ref. 5 and for $T_\infty = 1000^oK$ agreed to within 0.5% for $200 < Z < 2500$ km.

The relationship of T_∞, the exospheric temperature, to solar and geomagnetic activity will be discussed in the next section.

IV. ATMOSPHERIC PHENOMENA

Before discussing the various phenomena affecting the atmospheric properties a few words are in order as to the density measurements made in the last decade upon which the various phenomena have been correlated.

There are currently a number of experimental techniques that can be employed to measure the atmospheric density at high altitudes, however the method that has been employed almost exclusively in the past is based on an analysis of changes in satellite orbits. Over 100,000 density measurements of this type (i.e., density measurements based on satellite decay rates) have been performed to date. It has been estimated that errors in density of $\sim$ 9-13% exist[6] as the satellite decay rate technique is subject to a number of sources of error, some of which are described next. A satellite is influenced by a number of nonconservative forces in addition to drag, such as solar radiation presssure, terrestrial radiation pressure, non-neutral drag (i.e., electric drag due to charged particles), etc. that are in general treated as negligible. In the drag determination itself, however, there are two sources of uncertainty--the cross sectional area of the satellite S and the drag coefficient C_D. For the cross sectional area it is standard practice for a non-spherical configuration to assume that the body is tumbling and to employ an average cross sectional area that is based on tumbling motion. For an arbitrary body the average cross sectional area is 1/4 of the total surface area. Knowledge of

the drag coefficient is also uncertain and a value of $C_D = 2.2$ has been used as a 'standard' value irrespective of the body shape and/or surface material.[6] It should therefore be recognized that the density determination is based on these two assumptions and that therefore lifetime predictions should also be based on evaluating the ballistic coefficient with the same assumptions.

The major input to Jacchia's atmospheric model is the exospheric temperature T_∞. In Jacchia's latest report,[5] eight phenomena are listed that influence the value of T_∞, and empirical relations are presented that relate T_∞ to such factors as solar activity, seasonal variations, geomagnetic activity, etc. The eight phenomena currently recognized are classified by Jacchia as:

(1) Variations with the solar cycle

(2) Variations with the daily change in activity on the solar disk

(3) The diurnal variation

(4) Variation with geomagnetic activity

(5) The semiannual variation

(6) Seasonal-latitudinal variations of the lower thermosphere

(7) Seasonal-latitudinal variations of helium

(8) Rapid density fluctuations probably connected with gravity waves

These eight variations will be briefly described below. It should be kept in mind that we are primarily concerned with long lifetime estimates

($\lesssim$ 100 years) and that phenomena related to satellite position (latitude and longitude), date and/or time of day are too refined for our long term estimates and the phenomena will be discussed from this point of view.

1. Variation with solar cycle. The major variations of the high altitude atmospheric properties have been correlated over the years with the long term ($\sim$ 11 year) solar cycle. The mechanism by which this occurs is the absorption of Extreme UltraViolet (EUV) radiation (40Å to 1000Å) in the upper atmosphere by atomic oxygen. Since the radiation is completely absorbed it cannot be measured on the ground. Centimeter radiation, although in an entirely different spectral region is produced on the sun in processes related to those that produce the EUV radiation. This radiation is not absorbed by the atmosphere and can be detected and measured at ground level. It has been found that the 10.7 cm region of the centimeter radiation is highly correlated with the EUV radiation and easily measured. This centimeter radiation, $F_{10.7}$, is quoted in radiation units of 10^{-22} watts/m^2 H_z Ster and is measured daily at the Algonquin Radio Observatory at the National Research Council of Canada.

A second measure of solar activity is the relative sunspot number R_Z, which is measured at Zurich. It is determined each day and is essentially a visual count of the sunspots and the sunspot groups.

Shown in Table I are daily values, for a 12-month period, of R_Z and $F_{10.7}$ as reported in Ref. 7. The more quantitative index is, of course,

the $F_{10.7}$ cm flux. However, the $F_{10.7}$ cm flux has only been recorded since 1947. It will be shown later that the Zurich sunspot number, R_Z, and the level of $F_{10.7}$ cm flux are highly correlated.

Jacchia has empirically correlated the nighttime minimum global exospheric temperature, T_c, to the $\overline{F}_{10.7}$ cm flux averaged over three 27 day solar rotations,

$$T_c = 379 + 3.24\,\overline{F}_{10.7},\ ^{o}K \qquad (31)$$

In order to illustrate the effect of solar activity on upper atmospheric density, Fig. 1 shows results from Ref. 4 describing the density as a function of height for conditions of minimum and maximum solar activity. To be noted is the large variation in ρ above 400 km, one to two orders of magnitude, due to solar activity.

2. Variations with daily change in activity on the solar disk. Superimposed on Eq. (31) is a term $1.3\,(F_{10.7}-\overline{F}_{10.7})$ that accounts for density variations due to the short-time solar cycle based on the 27 day rotational period of the sun. In light of our long term orbital lifetime interests this term has been neglected, as suggested by Jacchia.[5]

3. Diurnal variation. This is the "day-to-night" effect, i.e., the difference between the dark side and sunlit side of the earth. Again the effect is due to the solar EUV radiation. The day-to-night temperature range is dependent on the latitude (large in low altitudes and decreases through the poles) and the seasons, following the migration of the subsolar point.

Jacchia gives empirical correlations relating the daytime maximum/nighttime minimum temperature ratio as a function of latitude, sun declination and local solar time. The maximum range is a ratio of 1.3. For the current studies we have assumed a linear average temperature between the maximum and minimum of 1.15 T_c, so that

$$T'_\infty = 1.15(379 + 3.24\ \overline{F}_{10.7}) \tag{32}$$

4. Variation with geomagnetic activity. It was noted that the earth's atmosphere reacts to magnetic disturbances caused by either magnetic storms originating on the sun due to solar flares or variations in the magnetic field of the earth. The physical processes causing the additional heating of the atmosphere due to magnetic fluxations are not known, however, it is observed that the energy dissipation varies with height and in the same height regime as does the EUV solar radiation effect. Again, Jacchia gives empirical correlations relating the change in exospheric temperature to the geomagnetic planetary index K_p, where by definition for $K_p = 0$ there is no magnetic effect. Based on Jacchia's[4] remarks we have selected $K_p = 2$ for an average quiet geomagnetic condition; this results in an exospheric temperature increase of 56^oK based on the results in Ref. 8. We therefore have

$$T_\infty = 1.15\ (379 + 3.24\ \overline{F}_{10.7}) + 56$$

or

$$T_\infty = 492 + 3.73\ \overline{F}_{10.7},\ ^oK\ . \tag{33}$$

5. The semiannual variation. A semiannual variation of atmospheric density with a time scale of half a year was detected in 1960. This variation occurs in the height range of 150 to 1100 km. The cause or mechanism of this variation is currently unknown. A density variation of $\pm$ 15% has been observed with a principal maximum in October, a principal minimum in July and a secondary maximum and minimum in April and January, respectively. Again Jacchia has proposed empirical correlations for the density variation as a function of altitude and time, however, over a cycle the average is defined as zero so that in our long term life time requirements this average of zero has been employed.

6. Seasonal-latitudinal variations of the lower thermosphere. This effect primarily influences the atmospheric density below 160 km. As our lifetime studies are completed when the satellite perigee attains $\sim$ 120 km this effect has been neglected.

7. Seasonal-latitudinal variations of Helium. A strong increase of helium concentration above the winter pole has been observed and it is felt that a seasonal migration of helium occurs, resulting in a seasonal variation of density. The effect has been deduced from satellite drag data and Jacchia has proposed an empirical correlation relating the change in helium concentration to the latitude and declination of the sun. As the variation is of a seasonal nature, i.e., relatively short characteristic time scale, this effect has been neglected.

8. Rapid density fluctuations probably connected with gravity waves. Density waves have been recently detected in the height range from 286 to 510 km with half amplitudes in density ranging from the limit of detectability to a maximum of about 50% of the mean density. The causes are unknown and insufficient data exists for a qualitative interpretation so that this effect has not been correlated by Jacchia.

V. THE 11 YEAR SOLAR CYCLE

As discussed in the previous sections the primary input to evaluating the upper atmospheric properties is the exospheric temperature T_∞, and in view of our specific interest in long lifetimes (tens of years and greater) a simple relationship, Eq. (33), has been established relating T_∞ to solar activity through the $\overline{F}_{10.7}$ cm solar flux. Unfortunately, a data base for the $F_{10.7}$ cm flux exists back to only 1947. However, historical records have provided investigators estimated values of R_z, the Zurich sunspot number, back to 1750, encompassing approximately 20 solar cycles.[9] The resulting yearly averages are shown in Fig. 2. Figure 3, adapted from Ref. 7, shows the monthly averages of R_z for the 18th, 19th and current 20th cycle (along with predictions of the 20th cycle) and the mean of cycles 8 thru 19 based on the values shown in Fig. 3. In order to use these Zurich sunspot data to estimate exospheric temperature, it now remains to relate R_z to $\overline{F}_{10.7}$ and in this respect we have employed the differences of the mean values of R_z and $F_{10.7}$ shown in Table I to give

$$F_{10.7} = R_z + 57 \tag{34}$$

Shown in Fig. 4 are the $F_{10.7}$ monthly averages from Table I and the values computed from Eq. (34) with the R_z values from Table I. As noted the correlation is adequate for our purpose. Assuming that Eq. (34) is valid for 3 month averages we have from Eqs. (33) and (34)

$$T_\infty = 492 + 3.73\ (\overline{R}_z + 57) \qquad (35)$$

where $\overline{R}_z$ is a 3 month average of the Zurich sunspot number. The $\overline{R}_z$ values employed in this study are taken from the mean curve shown in Fig. 3. The mean value of R_z, for the 11 year mean curve is $R_z = 52.4$ and from Eq. (35) this corresponds to a mean exospheric temperature $\overline{T}_\infty = 901^\circ K$. From the values shown in Fig. 2 we have evaluated the one σ variation of the peak values for the previous 19 cycles with a resulting one σ deviation of 37.5%. Assuming that the mean 11 year value ($R_z = 52.4$) will vary by the same percentage as the peak we find that a one σ variation of $\overline{T}_\infty$ is 8.1%.

VI. RESULTS

Comparison of Jacchia's tabular values[5] of density vs altitude to the 1962 standard atmospheric[4] values indicated that a value of $T_\infty = 1200^\circ K$ in the Jacchia atmosphere model yielded a close representation to the 1962 standard atmosphere. The resulting lifetime, L, calculations for $T_\infty = 1200^\circ K$ and for the 1962 standard atmosphere* are shown in Table II and

*The 1962 standard atmosphere was incorporated in tabular form in the computer code and as the values extend to only 700 km lifetime calculations were only possible for orbits with perigees < 465 km.

one notes the good agreement. Also shown in Table II are the effects of ballistic coefficient, β = 0.1, 1.0 and 4.0 and of arbitrary increasing the density by a factor of 10. The results are as expected in that the lifetime is directly proportional to ballistic coefficient and density. The comparison of β = 0.1 and 4 shows that there are no numerical problems with regard to precision and/or truncation.

At the onset of the study a number of questions were raised with regard to the 11 year solar cycle and some of these queries resulted in the calculations shown in Table III. It was suspected that if the lifetime were long (how long was not clear) that the lifetime estimates would correlate with the ballistic coefficient. Comparing the cases with β = 0.1, 1.0 and 2.0 it is found that this is correct and that a fair criteria is that the lifetime must be $\gtrsim$ 3 solar cycles (i.e., 12,000 days). The influence of where on the cycle one starts the lifetime calculations was also felt to be of small influence if the lifetimes were long. Again reference is made to Table III, where for β = 1 are shown lifetimes where in one case the calculations were initiated at the minimum (MIN) of the cycle and in a second case the calculations were initiated at the peak (MAX) of the cycle. It is found that if the lifetime is $\gtrsim$ 3 solar cycles the point at which one starts on the cycle is of small influence.

A third query concerned the applicability of employing a mean value of T_∞ as being representative of the 11 year mean solar cycle for the purpose of computing long term lifetimes. As noted in Table III it

is found that the mean value of $T_\infty = 901^\circ K$ (see Sect. V above) is not a valid representation of the 11 year cycle for use in lifetime studies. Since the lifetimes are directly proportional to density it was decided that rather than employ a time average value of T_∞ that it would be more appropriate to use a time average value of density for the 11 year mean cycle and determine the corresponding T_∞. This was done for altitudes from 200 to 2000 km and the resulting values of T_∞ are shown in Fig. 5. As the long lifetimes will occur for the higher perigee altitudes a value of $T_\infty = 955^\circ K$ was selected. As seen in Table III for lifetimes $\gtrsim$ 3 solar cycles the $T_\infty = 955^\circ K$ lifetimes are within 4% of the mean solar cycle values. This conclusion permits the relatively inexpensive derivation of a lifetime chart as will be described later.

Another question concerned the effect of uncertainties of the mean solar cycle on the lifetime estimates. Employing the one σ deviation of R_z from Sect. V, $\sigma = 37.5\%$, lifetime runs were made for a $\pm 1\ \sigma$ deviation and the results are shown in Fig. 6 along with the values for $T_\infty = 955^\circ K$ and $T_\infty = 1200^\circ K$ (i.e., the 1962 standard atmosphere). Restricting our attention to the long lifetimes ($\gtrsim$ 3 solar cycles) a factor of three difference in lifetimes is found from the $+ 1\ \sigma$ to the $- 1\sigma$ deviation. Again referring to Fig. 6 and comparing the $T_\infty = 955^\circ K$ values to the $T_\infty = 1200^\circ K$ values it is concluded, for long lifetimes, that lifetimes evaluated with the 11 year mean solar cycle ($T_\infty = 955^\circ K$) are a factor of ~ 4 greater than lifetimes evaluated with the 1962 standard atmosphere ($T_\infty = 1200^\circ K$).

As a further comparison and check of the computer code the lifetimes for a 200 n.m. circular orbit (e = 0) was calculated. Employing the $T_\infty = 1200^\circ K$ (i.e., the 1962 standard atmosphere equivalent) a lifetime of $L/\beta = 9.1$ days/(kg/m^2), resulted, which compares to within a percent of the results in Ref. 2. Using the 11 year solar cycle with $\beta = 10{,}000\ kg/m^2$ a $L/\beta = 27.1$ resulted and employing $T_\infty = 955^\circ K$ with $\beta = 1\ kg/m^2$ gave $L/\beta = 24.0$, a difference of 13%. Again it is concluded that the $T_\infty = 955^\circ K$ approximation to the 11 year cycle yields good results. For this case the lifetime based on the solar cycle is a factor of ~ 3 greater than the 1962 standard atmosphere value.

Based on the above results it is concluded that the $T_\infty = 955^\circ K$ Jacchia atmospheric model is a fairly good representation of the 11 year mean solar cycles for lifetimes $\lesssim 3$ solar cycles. Therefore it was decided to generate a lifetime chart based on $T_\infty = 955^\circ K$. Selection of a constant T_∞ model results in a drastic reduction in computer costs since small values of β can be employed to determine the ratio L/β. This result can then be used as an approximation to calculations based on the 11 year mean solar cycle for $L \lesssim 30$ years. The resulting lifetime chart for values of $e_o = 0.0$ to 0.90 to increments of 0.10 and for perigee altitudes from 200 to 1600 km is shown in Fig. 7.

The current results are compared in Fig. 8 to lifetime estimates taken from Ref. 1 and those based upon the 1962 standard atmosphere (i.e., the Jacchia model with $T_\infty = 1200^\circ K$). The estimates of Billik are based on an atmospheric model formulated by Billik.[10] The values of Kork are based on

the 1959-ARDC atmosphere and extend to a perigee altitude of 650 km. As noted the Kork and Billik estimates are in agreement. However, the lifetime estimates based on the 1962 standard atmosphere (which have been shown to agree with the lifetime estimates in Ref. 2 where comparisons are possible, i.e., below 550 km) are substantially higher, over an order of magnitude, for a large region. At the higher perigee altitudes, $\sim$ 1400 km, the Billik values are higher. Comparing the current estimates based on a mean value of $T_\infty = 955^\circ K$ as representative of the mean 11 year solar cycle, the discrepancy is larger, amounting to a factor of $\sim$ 60 for $e_o = 0$ at $h_p = 800$ km.

VII. CONCLUSIONS

A computational procedure has been developed that yields, for long ($>$ 30 years) satellite lifetimes, a fairly accurate estimate of the lifetime. The resulting computer code is both small and inexpensive to run. Based on the results reported above it can be concluded for long lifetimes that,

1) Lifetimes based on consideration of a mean solar cycle are a factor of 3 to 4 greater than lifetimes based on the 1962 standard atmosphere.
2) Long lifetimes are insensitive to where on the solar cycle the calculations are commenced.
3) Long lifetime estimates correlate with L/β.
4) Lifetime estimates for a one σ deviation of the mean solar cycle based on historical records are uncertain by a factor of $\sim$ 1.50.

5) Long lifetime estimates based on a constant exospheric temperature, derived from a time averaged value of density, yields a good estimate of lifetimes predicted using a time varying density based on the 11 year mean solar cycle.

For short lifetimes ($<$ 10 years) the graphical procedure developed in Ref. 2 is recommended. For medium lifetimes (10-30 years) the procedure outlined herein is recommended, however, rather than employ a mean solar cycle or a constant value of T_∞ it is suggested that solar cycle predictions be attempted for the next two solar cycles. It should be noted, in this regard that previous attempts at solar cycle predictions have been unsuccessful.[11] For long lifetimes ($>$ 30 years) the lifetime chart developed herein (Fig. 7) is recommended.

REFERENCES

1. Jensen, J., Townsend, G. Kork, J. and Kraft, D., Design Guide to Orbital Flight, McGraw-Hill Book Co., Inc., New York, 1962.
2. McNair, A. R. and Boykin, E. P., "Earth Orbital Lifetime Prediction Model and Program," NASA Technical Memorandum, TMX-53385, Feb. 1, 1966.
3. King-Hele, D., Theory of Satellite Orbits in an Atmosphere, Butterworths, Inc., Washington, D. C., 1964.
4. U. S. Standard Atmosphere, 1962, U. S. Govt. Printing Office, Washington, D. C., Dec. 1962.
5. Jacchia, L. G., "Revised Static Models of the Thermosphere and Exosphere with Empirical Temperature Profiles," Smithsonian Astrophysical Observatory, Special Report SR-332, May 5, 1971.

6. Roemer, M., "Structure of theThermosphere and its Variations, Deduced from Satellite Decay," published in Physics of the Upper Atmosphere, Bologna, Italy, Editrice Compositori, 1971.

7. "Solar-Geophysical Data (prompt reports)," U. S. Dept. of Commerce, Number 342-Part 1, Feb. 1973.

8. Jacchia, L. G., "Recent Results in the Atmospheric Region Above 200 km and Comparisons with CIRA 1965," Smithsonian Astrophysical Observatory, Special Report SR-245, July 7, 1967.

9. Hopfield, H., APL/JHU personal communication, The data for Fig. 2 were compiled from Refs. 7, 13, and 14.

10. Billik, B., "The Lifetime of an Earth Satellite," Aerospace Corp., TN-594-1105-1, Dec. 1960.

11. Vitinskii, Y. I., Solar-Activity Forecasting, Izdatel'Stvo Akademii Navk SSSR, Leningrad, 1962, Translation available from U. S. Dept. of Commerce, NASA TT F-289, TT 65-50115, 1965.

12. Abramowitz, M. and Stegun, J. A., eds., Handbook of Mathematical Functions with Formulas, Graphs, and Mathematical Tables, National Bureau of Standards, Applied Mathematics Series 55, U. S. Govt. Printing Office, Washington, D. C., Aug. 1966.

13. Menzel, D. H., Our Sun, Harvard University Press, 1959.

14. "Quarterly Bulletin on Solar Activity," International Astronomical Union.

NOMENCLATURE

a	=	Semimajor axis of the orbit, m
A	=	Avagardos number, 6.02257×10^{23}
C_D	=	Drag coefficient
C_n	=	Empirical constants, see Eq. (22)
D	=	Drag force, lb
e	=	Eccentricity of satellite orbit
E	=	Eccentric anomaly of the satellite
f_N	=	Force component normal to the orbital plane
f_T	=	Force component tangential to the orbital plane
F	=	See Eq. (10)
$F_{10.7}$	=	Solar centimeter radiation, 10^{-22} watts/m^2 Hz ster
g	=	Acceleration of gravity
H	=	Density scale height, m
i	=	Inclination of the orbit plane, deg
I_n	=	Bessell function
K_p	=	Geometric planetary index
L	=	Lifetime, days
m	=	Satellite mass, kg
$\mathfrak{m}$	=	Molecular weight, g/g-mole
N	=	Total number of particles per unit volume
r	=	Radius from earth's center, m
R	=	Universal gas constant, 8.31432 joules/(^{o}K-mole)

R_e = Earth radius, m

R_z = Zurich sunspot number

S = Cross sectional area of satellite, m^2

t = Time, sec

T = Temperature, ^oK

T_c = Nighttime minimum global exospheric temperature, ^oK

T_∞ = Exospheric temperature, ^oK

T_{500} = Temperature, ^oK, at Z = 500 km

v = Satellite inertial velocity, m/sec

V = Satellite velocity relative to V_A, m/sec

V_A = Air velocity, m/sec

Z = Altitude, km

α_i = Thermal diffusion coefficients for specie i

β = Ballistic coefficient, kg/m^2

γ = Flight path angle, deg

γ' = The angle between $\overline{V}_A$ and the horizontal component of $\overline{v}$, deg

η_i = Number density of i^{th} specie

θ = True anomaly of the satellite

λ = See Eq. (A7)

μ = Gravitational force constant

ξ = See Eq. (A4)

ρ = Density, g/m^3

σ = Standard deviation

ϕ = Geocentric latitude

ω = Angular velocity of earth, rad/sec

Subscripts

$( )_o$ = Initial conditions, also boundary conditions at Z_o = 90 km

$( )_p$ = Condition at perigee

$( )_{SL}$ = Conditions at sea level

$( )_x$ = Conditions at match point of the two temperature profiles

$( )_y$ = Boundary conditions at Z_y = 100 km

Superscripts

$\bar{( )}$ = Averaged value, also vector quantity

Table I. Relative Sunspot Numbers and Solar Flux Values for 1972 (from Ref. 7)

	1972 PROVISIONAL											1973
DAY	FEB	MAR	APR	MAY	JUN	JUL	AUG	SEP	OCT	NOV	DEC	JAN
1	53	74	48	17	78	68	93	121	78	78	35	45
2	52	89	46	39	96	74	81	91	65	67	23	53
3	39	96	43	32	102	85	85	69	73	49	20	55
4	46	84	38	27	116	91	80	68	73	26	20	60
5	49	72	32	49	132	104	93	77	67	19	18	72
6	48	64	51	68	103	92	85	78	57	16	18	83
7	49	74	76	79	95	97	65	73	54	8	24	66
8	99	84	75	73	87	86	56	65	52	7	33	68
9	96	81	74	99	76	75	59	57	30	14	42	70
10	97	81	88	91	68	64	44	43	24	12	51	55
11	97	68	75	79	63	62	25	43	26	38	59	52
12	62	88	88	92	48	77	50	33	16	26	60	32
13	73	91	78	103	43	89	55	31	14	25	63	35
14	89	104	65	130	68	86	37	35	8	27	60	15
15	108	114	67	113	88	61	39	42	14	18	64	18
16	137	104	60	125	98	60	57	53	34	25	66	11
17	137	114	55	140	101	59	62	44	30	32	76	27
18	146	110	59	133	86	55	52	35	28	21	51	42
19	162	112	62	127	83	73	54	38	44	36	38	47
20	159	113	65	105	92	59	48	44	45	54	54	60
21	156	110	85	89	96	70	60	60	53	58	70	62
22	167	113	85	77	87	72	85	69	63	62	57	62
23	141	119	83	59	84	68	71	59	66	68	60	60
24	128	119	82	58	79	64	82	71	81	65	43	58
25	93	112	88	56	77	62	64	82	91	54	39	39
26	88	55	88	55	73	83	79	78	95	52	32	27
27	79	34	62	41	66	82	89	77	103	51	31	8
28	88	25	66	44	78	86	113	67	84	58	26	14
29	91	29	38	58	73	106	147	78	65	40	20	7
30		42	22	79	73	112	141	75	90	37	29	16
31		37		85		115	137		84		37	13
MEAN	91.6	84.8	64.3	78.1	83.4	78.6	73.8	61.3	54.8	37.6	42.5	42.2

1971 yearly mean = 66.6

DAILY SOLAR FLUX AT 2800 MHz
OTTAWA ARO

FLUX ADJUSTED TO 1 A.U., S_a

	1972											1973
DAY	FEB	MAR	APR	MAY	JUN	JUL	AUG	SEP	OCT	NOV	DEC	JAN
1		125.5	96.8	95.8	128.2	133.8	156.3	144.3	114.7*	129.9	91.1	93.9
2	186.5	129.7	97.3	94.9	130.8	137.0	150.4	139.7*	108.4*	121.8*	89.4	98.2
3	184.8	131.1	98.1	97.7	137.5*	139.9	147.1*	129.4*	107.3	113.9	85.2	105.1*
4	183.6	137.1	101.8	102.7	149.5*	146.7*	146.8	122.8	103.3	115.8	82.3	109.3*
5	182.6	140.8	105.3	108.7	164.8	150.2	146.5	117.8*	100.6	102.6	80.4	113.3
6	98.6	143.7	118.1	117.6	159.1	146.1	143.4	119.2	98.4	93.2	77.8	115.8
7	102.2	143.3	121.3	120.9*	152.7	143.2	139.8*	110.4	96.1	85.7	87.1	112.3
8	104.3	141.6	123.8	126.8*	150.2*	136.7	125.3	115.9	97.2	82.5	91.6*	103.2
9	106.3	137.4	130.5	133.8	149.1*	127.1	123.8	112.9	100.5	82.3	94.7*	103.7
10	113.6*	132.5*	130.3	138.3	139.5	121.7	118.6	107.2	94.7	84.7	97.2*	103.8
11	118.4	134.9	129.8	140.8*	143.2*	123.6*	113.3*	102.7	93.5*	88.3	105.1*	102.8
12	123.9	128.5	128.3	148.6	149.7	119.3	107.6	100.6	94.7	88.7	108.9	103.5
13	126.3	129.3	128.4*	161.6	138.9*	119.9*	101.7	94.6	94.5	86.7	111.2*	100.9*
14	136.7	129.7	125.8	162.8	136.5	119.5	97.9	99.5	97.0	85.1	114.8*	96.2
15	145.8	135.3	126.0	164.6	139.5*	117.6	97.6	103.4	102.1*	86.5	116.1*	94.6
16	153.2	133.0	124.3	161.8	142.7*	115.1	100.6	103.1	106.2	89.6	110.2	93.8
17	168.2	133.8	120.3	169.3	149.6	114.6*	106.4	100.3	112.1*	91.5	111.9	94.2
18	184.4*	131.9	115.7	165.5	149.0*	108.9	109.6	102.6	111.8	94.6	112.4	95.3
19	190.6	131.0	115.4	156.7	143.2*	108.9	116.2	106.2	117.1*	99.7	113.2	94.8
20	282.5*	135.2	111.3	152.3	142.8	110.9	117.9	113.2	122.2	109.4	111.4	98.3
21	189.6*	135.8	106.9	148.2	139.8*	111.7	119.5	113.4*	132.8*	109.3*	113.4*	97.9
22	188.4*	131.2	109.4	143.3	135.1	111.6	127.3*	119.4*	141.7	110.9*	107.9*	98.5
23	175.6	140.0*	108.4	135.2	130.7	109.6	122.9*	125.2*	151.2*	115.3*	106.2	97.2
24	164.2	126.6	110.2	135.5	128.5	109.5	122.6	126.8	156.5	115.4*	101.1	96.9
25	151.9	116.4	111.6	127.3	125.5	112.4	127.8	126.3*	171.8	112.7	103.3*	95.6
26	149.3*	110.5	109.9	116.3*	120.8	120.6	137.4*	122.5*	170.0*	108.6	97.7	95.3
27	148.3	104.1	109.0*	114.3	121.9*	127.2	144.1	118.3*	167.6*	102.3	97.6	93.4
28	133.2	101.1	103.2	110.8*	127.3	133.3*	147.2*	116.4	159.1*	97.5	91.9	91.7
29	138.9*	96.5	98.6	116.2	132.4	139.1	163.3*	115.2		92.7	92.8*	91.4
30		98.3	97.8	116.8	134.5	141.2*	163.3	118.5	144.6*	95.1	92.0*	89.7
31		95.7		122.5		150.2	154.2*		140.1*		94.3	87.7
MEAN	138.4	127.1	113.7	132.5	139.7	126.8	128.9	114.9	120.2	99.7	99.7	99.0

* adjusted for burst

Table II. Lifetime Calculations - Based on 1962 Standard Atmosphere and an Equivalent Jacchia Atmosphere

APOGEE = 5000 km

Perigee km	1962 Std. ATM	T_∞ = 1200°K, Jacchia Atmosphere (1971)			
	β=1 L/β	β=1 L/β	β=0.1 L/β	β=4 L/β	β=1 ρ_R=10 L · ρ_R/β
200	10.2	10.2	10.9	10.1	10.9
250	30.8	30.8	31.8	30.8	31.8
350	179.3	170.5	172.0	170.3	172.0
450	750.3	721.7	723.7	721.5	723.7
550	2650.3	2659	2662	2659	2662
650	--*	8609	8612	8609	8612
750	--*	23908	23911	23907	23911

L → Lifetime, days

β → Ballistic coefficient, kg/m^2

ρ_R → Density ratio

*Tabular values of the 1962 standard atmosphere extend to only 700 km.

Table III. Lifetime Calculations - Jacchia Atmosphere

APOGEE = 5000 km

Perigee km	T_∞ =901°K β=1 L/β	Solar Cycle MIN β=1 L/β	Solar Cycle MAX β=1 L/β	Solar Cycle β=0.1 L/β	Solar Cycle β=2 L/β	T_∞ =955°K β=1 L/β
200	15.2	22.4	12.1	23.3	22.4	13.9
250	57.1	103.4	40.2	104.7	102.6	49.6
350	477.3	790.6	286.0	1261.0	554.1	378
450	2941	1872	3266	6690	2555	2151
550	14089	9964	11330	12473	10693	9932
650	51680	37287	36572	29737	36902	35841
750	135600	98257	99638	96280	98975	97765

L → Lifetime, days

β → Ballistic coefficient, kg/m^2

MAX → Start at minimum of solar cycle

MIN → Start at peak of solar cycle

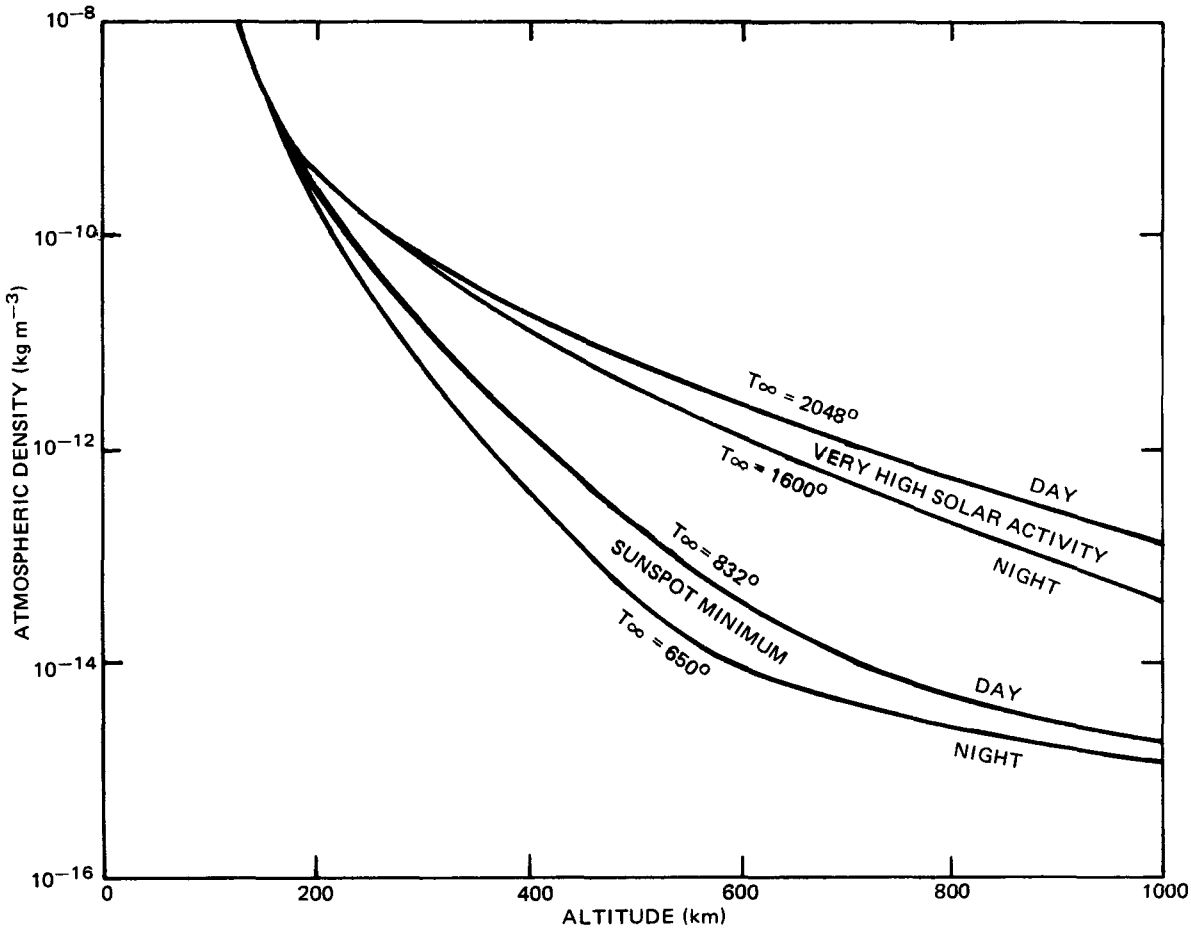

Fig. 1 DAY AND NIGHT DENSITY PROFILES IN THE UPPER ATMOSPHERE AT SUNSPOT MINIMUM AND AT A TIME OF EXCEPTIONALLY HIGH SOLAR ACTIVITY (FROM REF. 4)

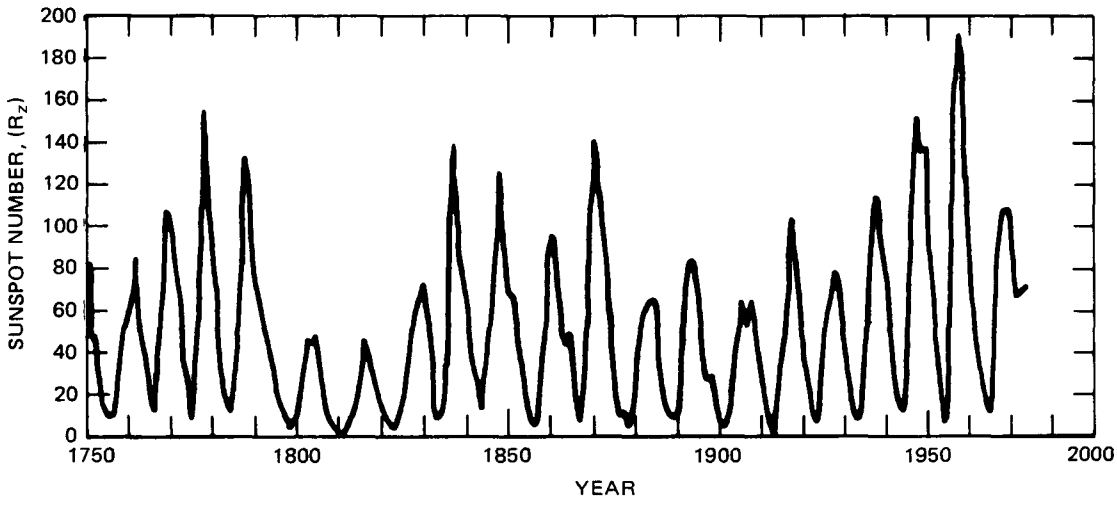

Fig 2 ZURICH RELATIVE SUNSPOT NUMBER YEARLY AVERAGES FROM 1749 TO 1972

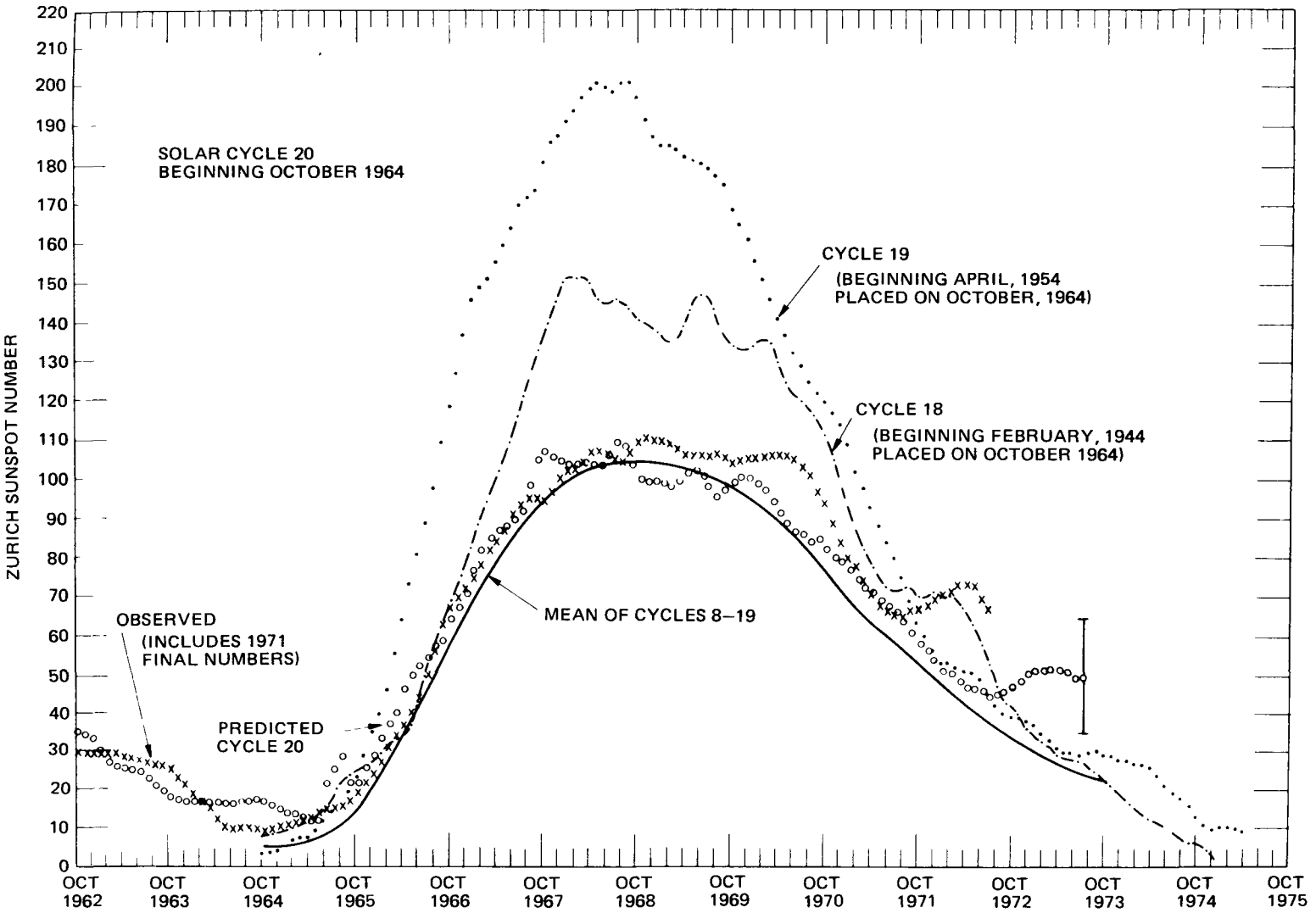

Fig. 3 PREDICTED AND OBSERVED SUNSPOT NUMBERS (FROM REF. 7)

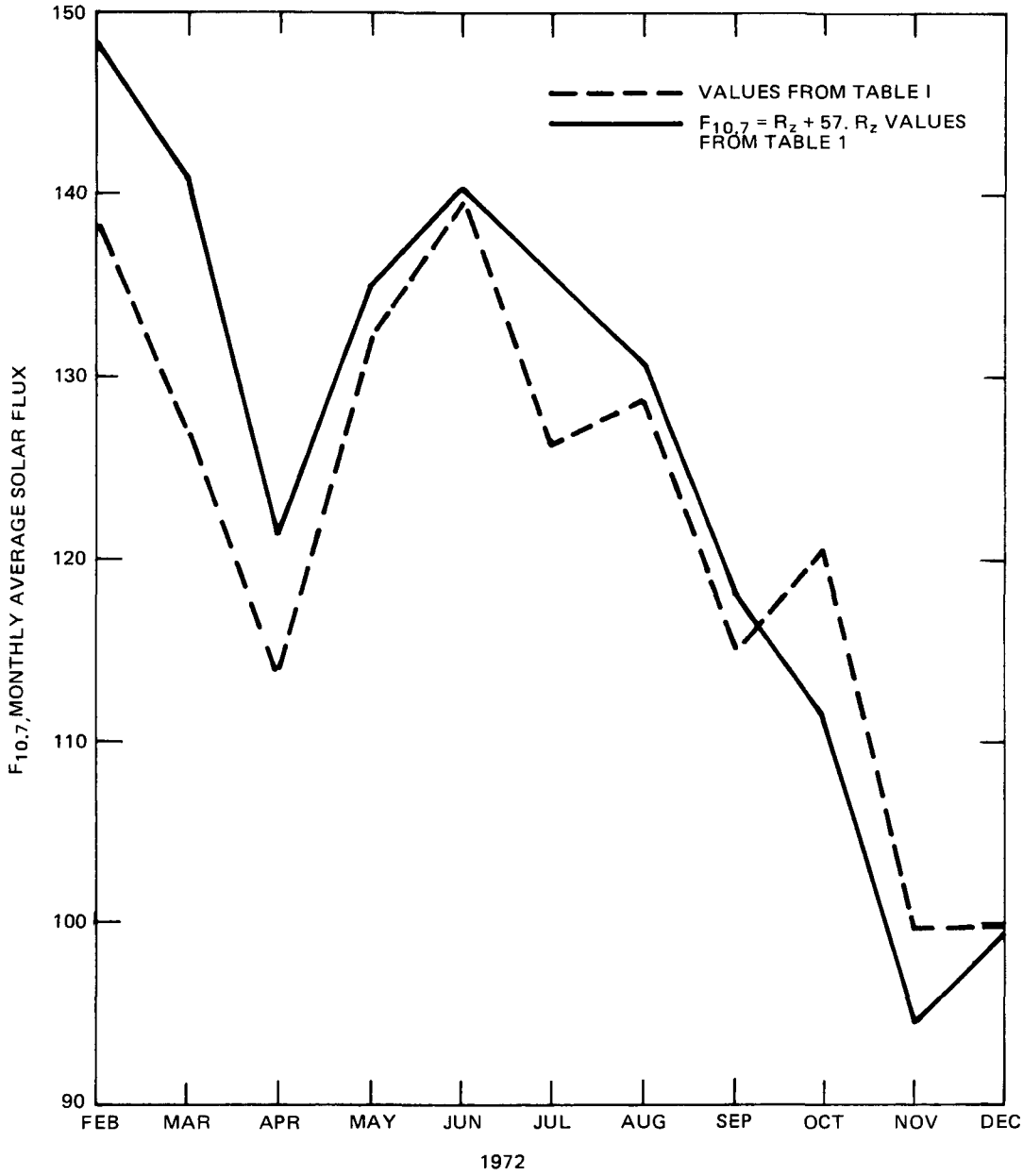

Fig. 4 COMPARISON OF MEASURED FLUXES TO VALUES COMPUTED WITH R_z

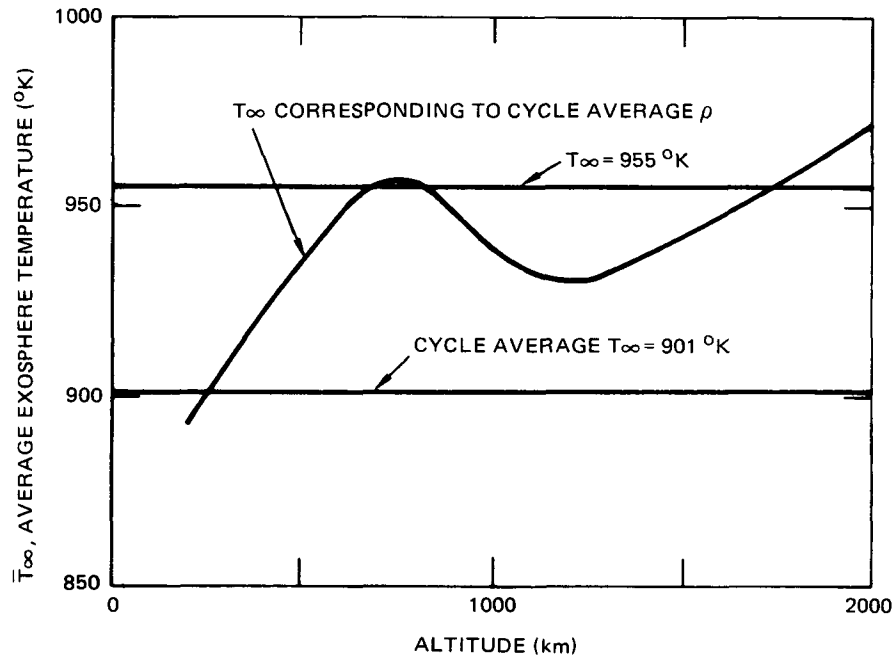

Fig. 5 AVERAGE EXOSPHERE TEMPERATURE BASED ON THE AVERAGE VALUE OF DENSITY FOR THE MEAN 11 YEAR SOLAR CYCLE

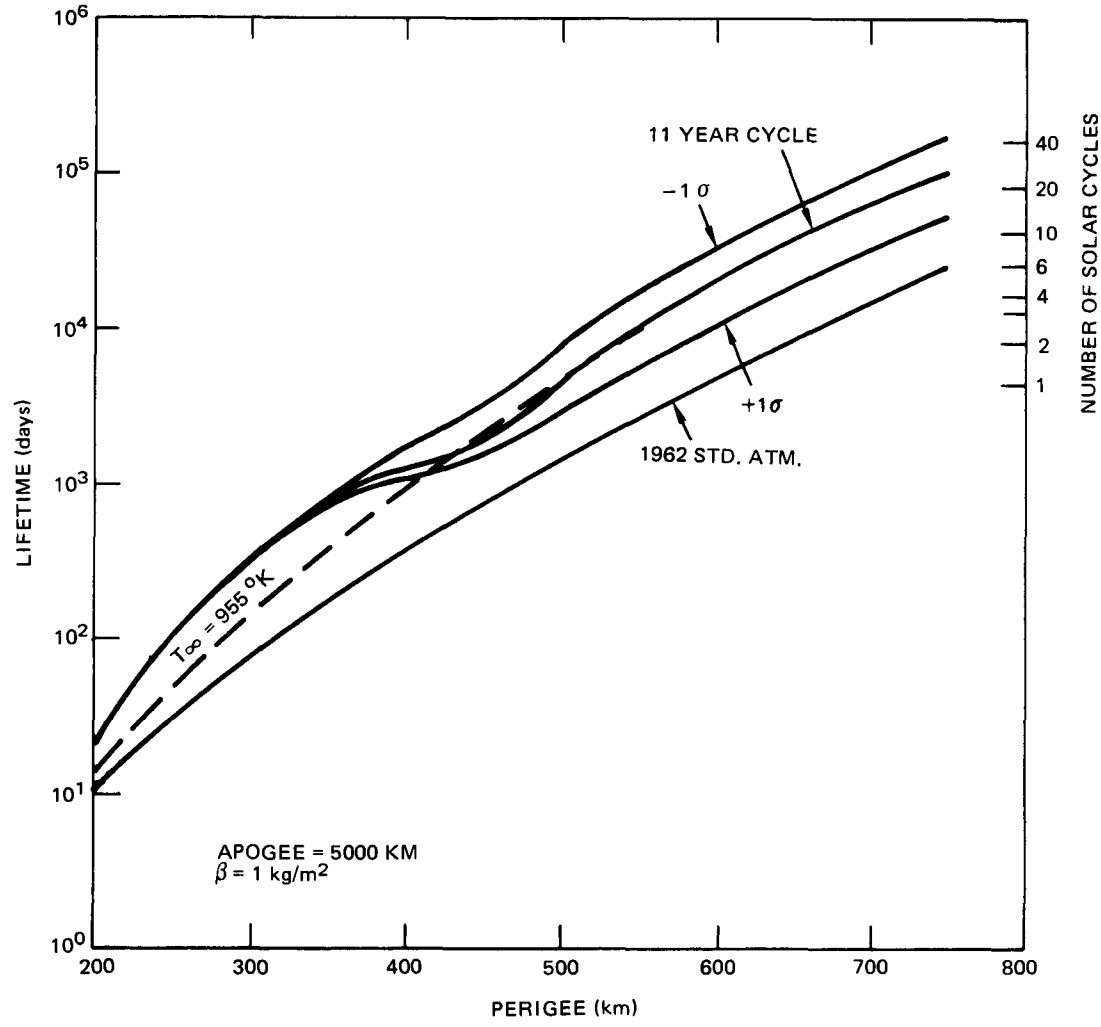

Fig. 6 LIFETIME ESTIMATES BASED ON SOLAR CYCLE COMPARED TO ESTIMATES BASED ON THE 1962 STANDARD ATMOSPHERE

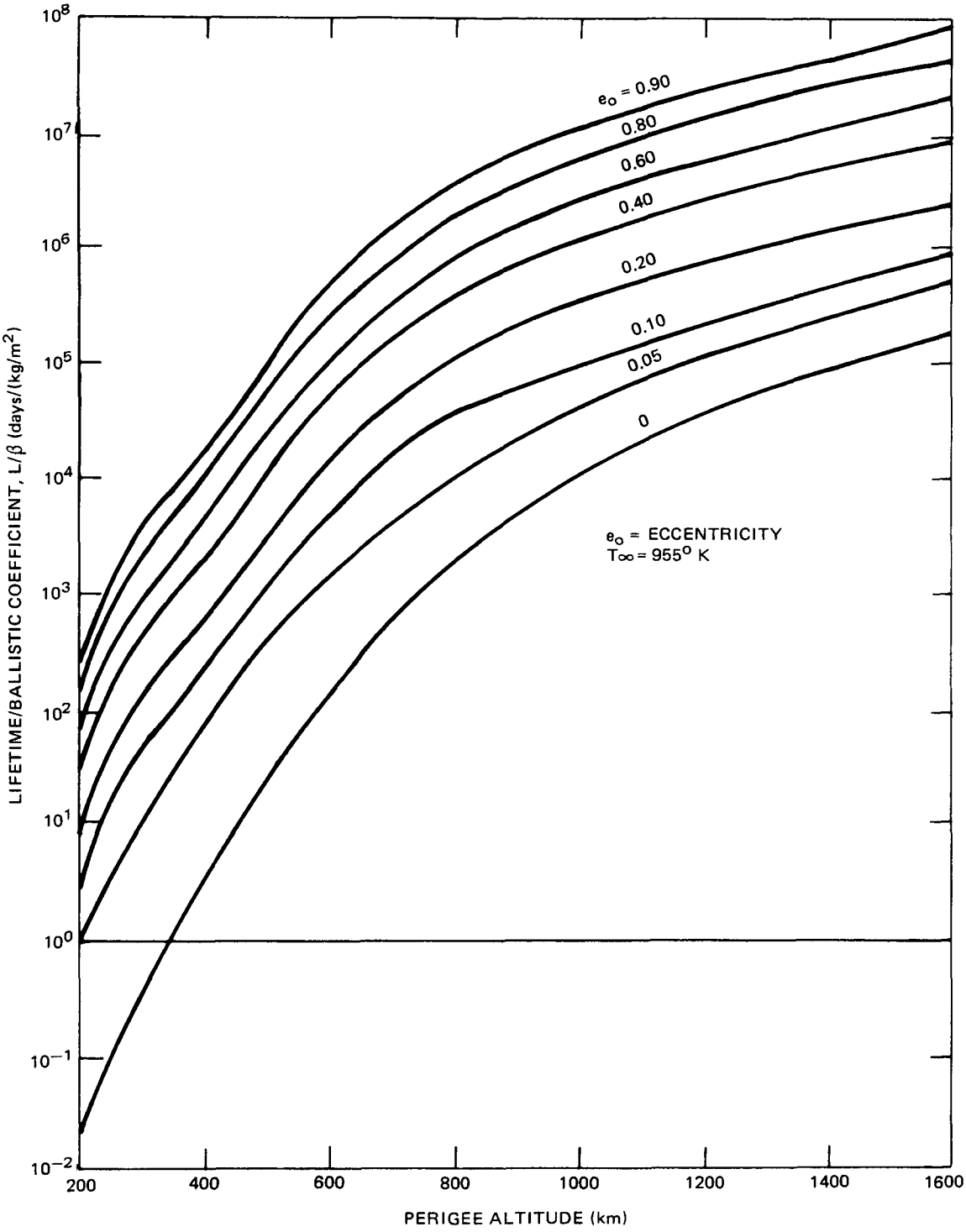

Fig. 7 ORBITAL LIFETIME MAP FOR LONG(>30YEARS) LIFETIMES BASED ON THE 11 YEAR MEAN SOLAR CYCLE

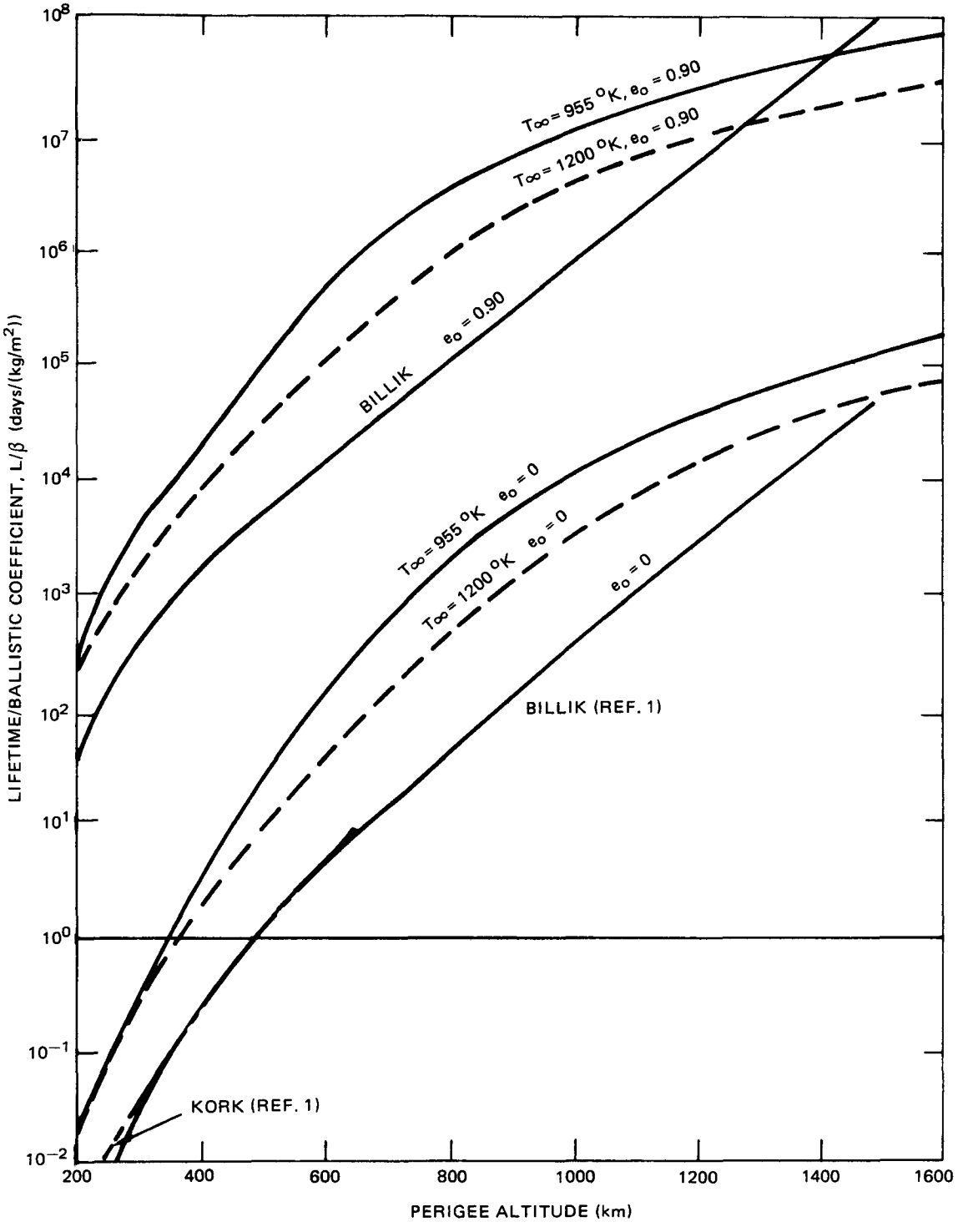

Fig. 8 COMPARISON OF LIFETIME ESTIMATES

THE JOHNS HOPKINS UNIVERSITY
APPLIED PHYSICS LABORATORY
SILVER SPRING MARYLAND

APPENDIX

Derivation of Equations of Motion

Details of the derivation for Δa will be presented; the $\Delta(ae)$ derivation is similar. Combining Eqs. (17) and (20) gives

$$\Delta a = -\frac{a^2}{\beta}\rho_p\, e^{\frac{a_o - a - a_o e_o}{H}} \int_o^{2\pi} \frac{(1 + e\cos E)^{3/2}}{(1 - e\cos E)^{1/2}}\, e^{-\frac{a\, e\cos E}{H}}\, dE \qquad \text{(A1)}$$

The binominal expansion is

$$(x + y)^n = 1 + nyz^{-1} + \frac{n(n-1)}{2!}\, y^2\, x^{-2} + \frac{n(n-1)(n-2)}{3!}\, y^3 x^{-3} \ldots \qquad \text{(A2)}$$

For the case $e < 0.2$ the expansion is performed in powers of e,

$$F \equiv (1 + e\cos E)^{3/2}\,(1 - e\cos E)^{-1/2}$$

$$= 1 + 2\, e\cos E + \frac{3}{2}\, e^2\cos^2 E + e^3\cos^3 E + \ldots$$

Therefore:

$$\Delta a = \frac{a^2}{\beta}\rho_p e^{\frac{a_o - a - a_o e_o}{H}} \left\{ \int_o^{2\pi} e^{-\frac{ae\cos E}{H}}\, dE + \int_o^{2\pi} 2e\cos E\, e^{-\frac{ae\cos E}{H}}\, dE \right.$$

$$\left. + \int_o^{2\pi} \frac{3}{2}\, e^2\cos^2 E\, e^{-\frac{ae\cos E}{H}}\, dE + \int_o^{2\pi} e^3\cos^3 E\, e^{-\frac{ae\cos E}{H}}\, dE + \ldots \right\}$$

Employing the trigometric identities

$$\cos^2 E = \frac{1}{2}\,(1 + \cos 2E)$$

$$\cos^3 E = \frac{1}{4}\,(\cos 3E + 3\cos E)$$

and the Bessell functions

$$I_n(\xi) = \frac{1}{2\pi} \int_0^{2\pi} \cos nE \; e^{\xi \cos E} \, dE \tag{A3}$$

where

$$\xi = ae/H \tag{A4}$$

we have finally

$$\Delta a = -\frac{2\pi a^2}{\beta} \rho_{p_o} e^{\frac{a_o - a - x_o}{H}} \left[I_0 + 2e\, I_1 + \frac{3}{4} e^3 (I_0 + I_2) + \frac{1}{4} e^3 (3I_1 + I_3) + \ldots \right] \tag{A5}$$

The corresponding relationship for Eq. (18) is

$$\Delta(ae) = -\frac{2\pi a^2 \rho_{p_o}}{\beta} e^{\frac{a_o - a - x_o}{H}} \left[I_1 + \frac{1}{2} e (3 I_0 + I_2) + \right.$$

$$\left. \frac{1}{8} e^2 (11 I_1 + I_3) + \frac{1}{16} e^3 (7 I_0 + 8 I_2 + I_4) + \ldots \right] \tag{A6}$$

For large values of e we make the substitution

$$\cos E = 1 - \lambda^2/\xi \tag{A7}$$

or

$$E = \cos^{-1} (1 - \lambda^2/\xi)$$

$$dE = \sqrt{2}\, d\lambda / \sqrt{\xi \left[1 - \lambda^2/(2\xi)\right]} \tag{A8}$$

Substituting Eqs. (A7) and (A8) into (A1) we have,

$$\frac{\Delta a}{-2\delta a^2 \rho_{p_o} e^{\frac{a_o - a - x_o}{H}}} = \sqrt{\frac{2}{\xi}} \int_o^{2\xi} \frac{\left[1 + e\left(1 - \frac{\lambda^2}{\xi}\right)\right]^{3/2}}{\left[1 - e\left(1 - \frac{\lambda^2}{\xi}\right)\right]^{1/2}} \frac{e^{\xi}\left(1 - \frac{\lambda^2}{\xi}\right)}{\left(1 - \frac{\lambda^2}{2\xi}\right)^{1/2}} d\lambda \tag{A9}$$

Again, employing the binominal expansion, Eq. (A2), we have for

$$F \equiv \left[1 + e\left(1 - \frac{\lambda^2}{\xi}\right)\right]^{3/2} \left[1 - e\left(1 - \frac{\lambda^2}{a}\right)\right]^{-1/2} \left(1 - \frac{\lambda^2}{2\xi}\right)^{-1/2}$$

or

$$F = (1 + e)^{3/2}(1 - e)^{-1/2} \left(1 - \frac{3}{2}\frac{e}{1 + e}\frac{\lambda^2}{\xi} + \frac{3}{8}\frac{e^2}{(1 + e)^2}\frac{\lambda^4}{\xi} + \ldots\right)$$
$$\left(1 - \frac{1}{2}\frac{e}{1 - e}\frac{\lambda^2}{\xi} + \frac{3}{8}\frac{e^2}{(1 - e)^2}\frac{\lambda^4}{\xi^2} + \ldots\right) \left(1 + \frac{1}{4}\frac{\lambda^2}{\xi} + \frac{3}{32}\frac{\lambda^4}{\xi^2} + \ldots\right)$$

Multiplying out and collecting terms we have

$$F = \frac{(1 + e)^{3/2}}{(1 - e)^{1/2}} \left[1 - \frac{\lambda^2(8e - 3e^2 - 1)}{4\xi\,(1 - e^2)} + K_1 \frac{\lambda^4}{\xi^2} + \ldots\right] \tag{A10}$$

where

$$k_1 = \frac{3 - 16e + 50e^2 + 16e^3 - 5e^4}{32\,(1 + e)^2\,(1 - e)^2} \tag{A11}$$

Substituting Eq. (A10) in Eq. (A9) and rearranging we find

$$\Delta a = -\frac{2a^2 \rho_{p_o} e^{\left(\frac{a_o - a - x_o}{H} + \xi\right)}}{\beta} \left(\frac{2}{\xi}\right)^{1/2} \frac{(1 + e)^{3/2}}{(1 - e)^{1/2}} \int_o^{2\xi} \left(1 - \frac{8e - 3e^2 - 1}{4\xi(1 - e^2)}\lambda^2 + \frac{k_1}{\xi^2}\lambda^4 + \ldots\right)$$
$$e^{\lambda^2} d\lambda \tag{A12}$$

The term by term integrations are performed by noting that $\sqrt{2\xi} > 6$ and therefore we can replace upper limit by ∞ for which we have

$$\int_o^\infty e^{-\lambda^2}\, d\lambda = \frac{\sqrt{\pi}}{2}$$

$$\int_o^\infty \lambda^2 e^{-\lambda^2}\, d\lambda = \frac{1}{4}\sqrt{\pi} \qquad \text{(A13)}$$

$$\int_o^\infty \lambda^4 e^{-\lambda^2}\, d\lambda = \frac{3}{8}\sqrt{\pi}$$

We therefore finally have from Eq. (A12) and (A13)

$$\Delta a = -\frac{a^2 \rho_{p_o}}{\beta}\left(\frac{2\pi}{\xi}\right)^{1/2}\frac{(1+e)^{3/2}}{(1-e)^{1/2}}\, e^{\frac{r_{p_o} - r_p}{H}}\left\{1 - \frac{8e - 3e^2 - 1}{8\xi(1-e^2)} + \frac{3}{4}\,\frac{k_1}{\xi^2} + \ldots\right\} \qquad \text{(A14)}$$

Similarly for Eq. (18) we find

$$\Delta(ae) = -\frac{a^2 \rho_{p_o}}{\beta}\left(\frac{2\pi}{\xi}\right)^{1/2}\frac{(1+e)^{3/2}}{(1-e)^{1/2}}\, e^{\frac{r_{p_o} - r_p}{H}}\left\{1 - \frac{3 + e^2}{8\xi(1-e^2)} + \frac{3}{4}\,\frac{k_2}{\xi^2} + \ldots\right\} \qquad \text{(A15)}$$

where

$$k_2 = \frac{-5 + 32e - 14e^2 + 32e^3 + 3e^4}{32\,(1-e^2)^2} \qquad \text{(A16)}$$

For e = 0 we have directly from Eq. (A1)

$$\Delta a = -2\pi\,\frac{a^2}{\beta}\,\rho_p e^{\frac{a_o - a}{H}} \qquad \text{(A17)}$$

and, of course,

$$\Delta(ae) = 0 \tag{A18}$$

Equations (A5), (A6), (A14), (A15), (A17) and (A18) are employed in the computer code. Based on the results of King-Hele[3] we have retained only terms up to and including e^2 in Eqs. (A5) and (A6) and the last terms $\left(\frac{3}{4}\frac{k_1}{\xi 2} \text{ and } \frac{3}{4}\frac{k_2}{\xi 2}\right)$ have been neglected in Eqs. (A14) and (A15).

For the Bessell function I_0, I_1, I_2 and I_3 required in Eqs. (A5) and (A6) series approximations are employed for $\xi < 3$,[3]

$$I_0(\xi) = \frac{e^{\xi}}{\sqrt{2\pi\xi}}\left[1 + \frac{1}{8\xi} + \frac{9}{128\xi^2} + \ldots\right] \tag{A19}$$

$$I_1(\xi) = \frac{e^{\xi}}{\sqrt{2\pi\xi}}\left[1 - \frac{3}{8\xi} - \frac{15}{128\xi^2} + \ldots\right] \tag{A20}$$

For $\xi \geq 3$ we employ the empirical curve fits from Ref. 11

$$I_0(\xi) = 1.0 + 3.5156229\,\xi^2 + 3.0899424\,\xi^4 + 1.2067492\,\xi^6 + 0.2659732\,\xi^8 + 0.0360768\,\xi^{10} + 0.0045813\,\xi^{12} \tag{A21}$$

$$I_1(\xi) = \xi\left[0.50 + 0.87890594\,\xi^2 + 0.51498869\,\xi^4 + 0.15084934\,\xi^6 + 0.02658733\,\xi^8 + 0.00301532\,\xi^{10} + 0.00032411\,\xi^{12}\right] \tag{A22}$$

The values for I_2 and I_3 are found from the recurrence relations

$$I_0(\xi) - I_2(\xi) = \frac{2}{\xi} I_1(\xi) \tag{A23}$$

$$I_1(\xi) - I_3(\xi) = \frac{4}{\xi} I_2(\xi) \tag{A24}$$

THE JOHNS HOPKINS UNIVERSITY
APPLIED PHYSICS LABORATORY
SILVER SPRING MARYLAND

INITIAL DISTRIBUTION EXTERNAL TO THE APPLIED PHYSICS LABORATORY

ORGANIZATION	LOCATION	ATTENTION	No. of Copies
U. S. Atomic Energy Commission	Germantown, Md.	G. L. Bennett	1
		G. P. Dix	1
		T. J. Dobry	1
		N. Goldenberg	1
		H. Jaffe	1
		J. J. Lombardo	1
		W. C. Remini	1
Air Force Weapons Laboratory	Albuquerque, N.M.	Capt. D. Egan	1
		Lt. D. L. Tate	1
NASA/Ames	Moffett Field, Calif.	J. W. Vorreiter	1
NASA/Langley	Hampton, Va.	G. D. Walberg	1
Los Alamos Scientific Laboratory	Los Alamos, N.M.	R. N. R. Mulford J. Burns	1
Oak Ridge National Laboratory	Oak Ridge, Tenn.	R. G. Donnelly	1
Aerospace Corporation	Los Angeles, Calif.	J. C. Bailey	1
AVCO Systems Division	Wilmington, Mass.	P. Levine	1
General Electric Co.	King of Prussia, Pa.	D. D. Knight	1
		C. T. Bradshaw	1
Donald W. Douglas Laboratory	Richland, Wash.	J. D. Watrous	1
Fairchild Industries	Germantown, Md.	H. P. Kling	1
TRW Systems, Inc.	Redondo Beach, Calif.	J. M. Bell	1
Westinghouse Electric Corp.	Pittsburgh, Pa.	W. G. Parker	1